Segmental Mobility in Phosphorus-Containing Dendrimers. Studies by Fluorescent Spectroscopy

Laurent Brauge,[†] Anne-Marie Caminade,[†] Jean-Pierre Majoral,[†] Stanislaw Slomkowski,*[,‡] and Marian Wolszczak[§]

Laboratoire de Chimie de Coordination du CNRS, 205 route de Narbonne, 31077 Toulouse 4, France; Center of Molecular and Macromolecular Studies, Polish Academy of Sciences, Sienkiewicza 112, 90-363 Lodz, Poland; and Institute of Applied Radiation Chemistry, Technical University of Lodz, Wroblewskiego 15, 93-590 Lodz, Poland

Received November 27, 2000; Revised Manuscript Received May 14, 2001

ABSTRACT: Steady-state fluorescence spectra and decays of excitations of a phosphorus-containing dendrimer labeled with 12 internal labels and of an iminophosphorane model compound bearing two labels dissolved in acetonitrile, diglyme, 1,4-dioxane, triethylene glycol, and cyclohexanol revealed that the interior of dendrimers contained many solvent molecules, and movements of internally located pyrene labels were not reduced by interactions with the dendrimer core. This conclusion was based on the following findings. A ratio of the intensities of pyrene−pyrene excimer and pyrene monomer emissions (I_E/I_M) decreased with increasing solvent viscosity but, with exception of acetonitrile solutions, was very close for the dendrimers and for the model. Monomer and excimer emission intensity decays were fitted with two-exponential functions with time constants τ_1 and τ_2 characterizing formation of pyrene−pyrene excimers and recovery of pyrene moieties in their ground state, respectively. For solvent viscosities varying from 3.44×10^{-3} P (acetonitrile) to 4.78×10^{-1} P (triethylene glycol), τ_1 increased from 7.1 to 37.7 ns and from 6.2 to 34.9 ns for the model and for the dendrimer. In acetonitrile the rates of the pyrene−pyrene excimer formation were almost the same for the labels in solution and bound covalently in the interior of the dendrimer core. For more viscous solvents the extensive reduction of pyrene label mobility has been noticed for both the model and labeled dendrimer.

Introduction

The topology of dendrimers induces much higher crowding of atoms at the periphery of these macromolecules than in the areas close to their centers. We were interested in finding out to what extent the mobility of the relatively large pyrene moieties labeling internal branches of dendrimers is reduced by label interactions with other dendrimer segments. The answer to the above-mentioned question has basic and practical importance. Dendrimers are considered to be potentially useful as carriers of catalysts, bioactive compounds, and other interacting species. Action of dendrimeric carriers may consist of incorporation of small molecules followed by their binding in the dendrimeric active sites. Thus, it is important not only to find methods for synthesis of required reactive groups inside of dendrimers but also to learn whether mobility of these groups would be sufficient to allow for their orientation needed for complexation of incoming molecules.

Fluorescent spectroscopy was used as a method of choice for studies of distribution of small molecules between interior of dendrimers and a solvent,[1,2] for studies of controlled release of small molecules entrapped in dendrimers,[3] and also to obtain information on the mobility of fluorescent labels located at the exterior of the relatively rigid polyphenylene dendrimers.[4,5] Recently, some of us developed a convenient way to carry on reactions on internal segments of phosphorus-containing dendrimers leaving their external parts intact.[6] We wanted to use this strategy for synthesis of a dendrimer of generation 3 bearing 12 labels at the generation 0 level with hope to obtain an interesting model allowing to study internal mobility of synthesized dendrimers.

Experimental Part

The solvents acetonitrile, diglyme, 1,4-dioxane, triethylene glycol, and cyclohexanol were distilled, and their spectroscopic purity has been checked before using.

Synthesis of the Model Compound 4. The 1-pyrenebutyric hydrazide **1** and the thiophosphoazide **2** have been prepared according to the literature.[7,8] The azide labeled with pyrene groups **3** was synthesized by reacting an excess of 1-pyrenebutyric hydrazide **1** (0.630 g, 2.08 mmol) with the phosphorus azide (0.360 g, 1 mmol) in THF (10 mL). Then, solvent was partially removed under reduced pressure, and 1-pyrene-labeled phosphorus azide was precipitated with pentane and washed three times with water. Model compound **4** was obtained by reacting the labeled azide **3** (0.100 g, 0.109 mmol) with diphenylmethylphosphine (0.040 mL, 0.214 mmol) (cf. Scheme 1) in THF (5 mL) for 1 h at room temperature. Evaporation of the solvent left a brown oil which was washed with diethyl ether (3 × 10 mL) to give **4** as a pale brown powder (92% yield).

Structures indicating carbon atoms listed in NMR data are depicted in Scheme 1.

3: ^{31}P {^{1}H} NMR (THF, 32.438 MHz): δ 58.6. ^{1}H NMR (THF-d_8, 300.13 MHz): δ 2.29 (m, 4H, $CH_2CH_2CH_2$), 2.91 (t, $^3J_{HH} = 6.8$ Hz, 4H, CH_2−pyr), 3.51 (t, $^3J_{HH} = 7.2$ Hz, 4H, CH_2-CO), 7.26 (dd, $^3J_{HH} = 8.4$ Hz, $^4J_{HP} = 1.7$ Hz, 4H, H−C^2), 7.65 (d, $^3J_{HH} = 8.4$ Hz, 4H, H−C^3), 7.84 (s, 2H, C*H*=N), 7.97 (d, $^3J_{HH} = 7.9$ Hz, 2H, H−C$^{2'}$), 7.98 (m, $^3J_{H9H8} = 7.9$ Hz, $^3J_{H9H10} = 7.6$ Hz, 2H, H−C$^{9'}$), 8.04 (d, $^3J_{HH} = 8.9$ Hz, 2H, H−C$^{5'}$), 8.07 (d, $^3J_{HH} = 8.9$ Hz, 2H, H−C$^{6'}$), 8.14 (d, $^3J_{HH} = 9.3$ Hz, 2H, H−C$^{12'}$), 8.15 (d, $^3J_{HH} = 7.9$ Hz, 2H, H−C$^{8'}$), 8.18 (m, 4H, H−C$^{3'}$ and H−C$^{10'}$), 8.52 (d, $^3J_{HH} = 9.3$ Hz, 2H, H−C$^{13'}$), 10.43 (s, 2H, N*H*). ^{13}C {^{1}H} NMR (THF-d_8, 75.468 MHz): δ 27.91 (s, $CH_2CH_2CH_2$), 33.17 (s, CH_2−pyr), 34.10 (s, CH_2CO), 122.52 (d, $^3J_{PC} = 5.4$ Hz, C^2), 124.71 (s, C$^{13'}$), 125.63, 125.74, 125.79

[†] Laboratoire de Chimie de Coordination du CNRS.
[‡] Polish Academy of Sciences.
[§] Technical University of Lodz.

10.1021/ma0020077 CCC: $20.00
Published on Web 07/07/2001

Scheme 1. Preparation of the Pyrene Labeled Azide 3 and of the Model 4

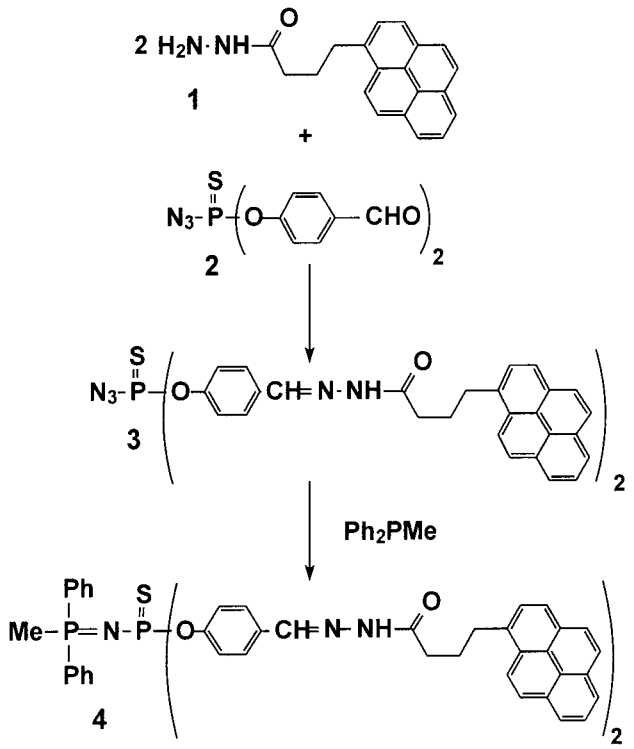

(3 s, $C^{3'}$, $C^{8'}$, $C^{10'}$), 126.10, 126.17 (2 s, $C^{15'}$, $C^{16'}$), 126.73 (s, $C^{9'}$), 127.49 (s, $C^{5'}$), 128.13 (s, $C^{12'}$), 128.46 (br s, $C^{2'}$, $C^{6'}$), 129.19 (s, C^{3}), 129.96 (s, $C^{14'}$), 131.10 (s, $C^{7'}$), 131.24 (s, C^{4}), 132.18 (s, $C^{11'}$), 132.63 (s, $C^{4'}$), 137.81 (s, $C^{1'}$), 141.32 (s, CH=N), 149.77 (d, $^2J_{CP}$ = 11.1 Hz, C^1), 175.11 (s, C=O). IR (KBr): ν = 2162 cm^{-1} (N_3). Anal. Calcd for $C_{54}H_{42}N_7O_4PS$ (916.00): C, 70.80; H, 4.62; N, 10.70. Found: C, 70.68; H, 4.55; N, 10.64.

4: $^{31}P\{^1H\}$ NMR ($CDCl_3$, 81.015 MHz): δ 16.42 (d, $^2J_{PP}$ = 33.0 Hz, P=N), 52.86 (d, $^2J_{PP}$ = 33.0 Hz, P=S). ^1H NMR ($CDCl_3$, 250.133 MHz): δ 2.23 (d, $^2J_{HH}$ = 13.2 Hz, 3H, CH_3P), 2.29 (m, 4H, $CH_2CH_2CH_2$), 2.87 (t, $^3J_{HH}$ = 7.2 Hz, 4H, CH_2−pyr), 3.43 (t, $^3J_{HH}$ = 6.6 Hz, 4H, CH_2CO), 7.18 (d, $^3J_{HH}$ = 8.1 Hz, 4H, H−C^2), 7.30−8.10 (m, 32H, HC=N, C_6H_5, H−C^3, pyrene), 8.32 (d, $^3J_{HH}$ = 9.3 Hz, 2H, H−$C^{13'}$), 9.77 (s, 2H, N*H*). $^{13}C\{^1H\}$ NMR ($CDCl_3$, 62.896 MHz): δ 14.44 (d, $^2J_{CP}$ = 67.4 Hz, CH_3P), 26.56 (s, $CH_2CH_2CH_2$), 32.38 (s, CH_2−pyr), 32.94 (s, CH_2CO), 121.77 (d, $^3J_{CP}$ = 4.1 Hz, C^2), 123.25 (s, $C^{13'}$), 124.6−125.0 (m, $C^{3'}$, $C^{8'}$, $C^{10'}$, $C^{15'}$, $C^{16'}$), 125.61 (s, $C^{9'}$), 126.44 (s, $C^{5'}$), 127.19 (br s, $C^{2'}$, $C^{6'}$, $C^{12'}$), 127.90 (s, C^3), 128.64 (d, $^3J_{CP}$ = 12.5 Hz, C_m), 129.69 (s, $C^{14'}$), 130.35 (s, $C^{7'}$), 130.42 (s, C^4), 130.80 (d, $^2J_{CP}$ = 11.1 Hz, C_o), 131.13 (s, $C^{11'}$), 132.29 (s, $C^{4'}$, C_p), 135.88 (s, $C^{1'}$), 142.66 (s, CH=N), 153.30 (d, $^2J_{CP}$ = 9.2 Hz, C^1), 175.82 (s, C=O); C_i not detected. Anal. Calcd for $C_{67}H_{55}N_5O_4P_2S$ (1088.21): C, 73.95; H, 5.09; N, 6.43. Found: C, 73.87; H, 4.98; N, 6.39.

Synthesis of the Dendrimer 11. Incorporation of pyrene labels within the cascade structure of a dendrimer necessitated first the activation of the new nonlabeled dendrimer **8** which was prepared according to the general strategy illustrated in Scheme 2.[6] To a solution of **8** (0.430 g, 27 μmol) in dichloromethane (15 mL) was added methyl triflate (20 μL, 177 μmol). After stirring 1 h, the solvent and the excess of methyl triflate were removed and the residue washed with diethyl ether (2 × 10 mL) to give the polycationic dendrimer **9** as a yellow powder (93% yield). To the yellow solution of dendrimer **9** (0.46 g, 27 μmol) in degassed THF (10 mL) was then added tris(dimethylamino)phosphine (40.8 μmol, 224.4 μmol). After stirring 3 h, the noncolored solution was evaporated to dryness under vacuum to give **10**, which was immediately treated with a degassed THF solution (10 mL) of the azide **3** (0.15 g, 0.50 mmol) to avoid oxidation of the generated aminophosphite groups. After stirring 1 h, the solvent was evaporated and the resulting brown powder washed with diethyl ether (3 × 10 mL) and then acetonitrile (2 × 5 mL) to give **11** as a slight brown solid in 88% yield (Scheme 2).

8: $^{31}P\{^1H\}$ NMR ($CDCl_3$, 81.015 MHz): δ = 8.1 (br s, P_0), 13.6 (d, $^2J_{PP}$ = 31 Hz, P_0'), 52.6 (d, $^2J_{PP}$ = 31 Hz, P_1), 60.4 (s, P_3), 62.5 (s, P_2). ^1H NMR ($CDCl_3$, 250.133 MHz): δ = 2.79 (s, 18 H, Me_0), 3.35 (m, 108 H, Me_1, Me_2), 4.74 (br s, 12H, NCH_2P), 6.75−7.85 (m, 462H, C_6H_4, C_6H_5, HC=N), 9.85 (s, 48H, CHO). $^{13}C\{^1H\}$ NMR ($CDCl_3$, 62.896 MHz): δ = 32.9 (br d, $^2J_{CP}$ = 14 Hz, Me_1, Me_2), 39.0 (s, Me_0), 56.9 (br d, $^1J_{CP}$ = 76 Hz, CH_2), 120.6 (s, C_0^2), 121.9 (d, $^3J_{CP}$ = 4 Hz, C_1^2, C_2^2, C_3^2), 126.6 (s, C_0^3), 128.1 (s, C_1^3), 128.3 (s, C_2^3), 128.6 (d, $^3J_{CP}$ = 13 Hz, C_m), 131.0 (s, $(HC=N)_0$ and C_1^4), 131.5 (s, C_3^3), 131.8 (s, C_2^4), 132.2 (d, $^2J_{CP}$ = 10 Hz, C_o), 132.7 (s, C_p), 133.4 (s, C_0^4), 133.6 (s, C_3^4), 139.7 (d, $^3J_{cp}$ = 14 Hz, $(HC=N)_1$ and $(HC=N)_2$), 149.6 (br s, C_0^1), 151.5 (d, $^2J_{CP}$ = 8 Hz, C_2^1), 152.8 (d, $^2J_{CP}$ = 8 Hz, C_1^1), 155.1 (d, $^2J_{CP}$ = 8 Hz, C_3^1), 190.8 (s, CHO); C_i not detected. Anal. Calcd for $C_{750}H_{648}N_{93}O_{138}P_{51}S_{42}$ (16098): C, 55.95; H, 4.05; N, 8.09. Found: C, 55.86; H, 3.98; N, 8.00.

9: $^{31}P\{^1H\}$ NMR ($CDCl_3$, 81.015 MHz): δ = 8.1 (br s, P_0), 20.1 (d, $^2J_{PP}$ = 9 Hz, P_1), 24.3 (d, $^2J_{PP}$ = 9 Hz, P_0'), 60.6 (s, P_3), 62.4 (s, P_2). ^1H NMR (CD_3COCD_3, 250.133 MHz): δ = 2.36 (d, $^3J_{HP}$ = 16.2 Hz, 18H, S-Me), 2.79 (s, 18 H, Me_0), 3.35 (m, 108 H, Me_1, Me_2), 4.74 (br s, 12H, NCH_2P), 6.75−7.85 (m, 462H, C_6H_4, C_6H_5, HC=N), 9.85 (s, 48H, CHO). $^{13}C\{^1H\}$ NMR ($CDCl_3$, 62.896 MHz): δ = 13.5 (br s, S-Me), 32.9 (bs d, $^2J_{CP}$ = 13 Hz, Me_1, Me_2), 39.7 (s, Me_0), 56.9 (br s, CH_2−P), 121.0 (s, C_0^2), 121.1 (d, $^3J_{CP}$ = 5 Hz, C_1^2), 121.8 (br s, C_2^2), 121.9 (d, $^3J_{CP}$ = 4 Hz, C_3^2), 128.4 (s, C_2^3, C_0^3), 128.5 (d, $^3J_{CP}$ = 11 Hz, C_m), 129.6 (s, C_1^3), 129.6 (br s, $(HC=N)_0$ and C_1^4), 131.5 (s, C_3^3), 131.8 (d, $^2J_{CP}$ = 8 Hz, C_o), 132.2 (s, C_2^4), 133.6 (s, C_3^4 and C_p), 133.8 (s, C_0^4), 139.3 (d, $^3J_{CP}$ = 14 Hz, $(HC=N)_1$), 139.8 (d, $^3J_{CP}$ = 13 Hz, $(HC=N)_2$), 149.8 (d, $^2J_{CP}$ = 11 Hz, C_1^1), 151.0 (d, $^2J_{CP}$ = 8 Hz, C_0^1), 151.5 (d, $^2J_{CP}$ = 11 Hz, C_2^1), 155.1 (d, $^2J_{CP}$ = 6 Hz, C_3^1), 190.8 (s, CHO); CF_3, C_i not detected. $^{19}F\{^1H\}$ NMR ($CDCl_3$, 198 MHz): δ = −1.96 (s, CF_3). Anal. Calcd for $C_{762}H_{666}F_{18}N_{93}O_{156}P_{51}S_{48}$ (17083): C, 53.57; H, 3.92; N, 7.62. Found: C, 53.45; H, 3.88; N, 7.57.

11: $^{31}P\{^1H\}$ NMR ($CDCl_3$, 81.015 MHz): δ = −12.5 (dd, $^2J_{P1P0'}$ = 21 Hz, $^2J_{P1P1'}$ = 64 Hz, P_1), 8.1 (br s, P_0), 13.4 (d, $^2J_{P1P0'}$ = 21 Hz, P_0'), 46.7 (d, $^2J_{P1P1'}$ = 64 Hz, P_1'), 60.4 (s, P_3), 62.4 (s, P_2). ^1H NMR ($CDCl_3$, 330.131 MHz): δ = 2.33 (m, 24H, $CH_2CH_2CH_2$), 2.72 (s, 18H, Me_0), 2.87 (t, $^3J_{HH}$ = 7.6 Hz, 24H, CH_2−pyr), 3.32 (m, 108H, Me_1, Me_2), 3.48 (t, $^3J_{HH}$ = 7.2 Hz, 24H, CH_2CO), 4.58 (br s, 12H, NCH_2P), 6.75−7.85 (m, 630H, C_6H_4, C_6H_5, $C_{16}H_9$, HC=N), 9.88 (s, 48H, CHO), 9.98 (s, 12H, N*H*). $^{13}C\{^1H\}$ NMR ($CDCl_3$, 62.896 MHz): δ = 26.7 (s, $CH_2CH_2CH_2$), 32.5 (s, CH_2−pyr), 32.9 (br d, $^2J_{CP}$ = 13 Hz, Me_1, Me_2), 33.0 (s, CH_2CO), 39.0 (br s, Me_0), 120.7 (s, C_0^2), 121.3 (d, $^3J_{CP}$ = 4 Hz, C^2), 121.9 (br s, C_1^2, C_2^2, C_3^2), 123.3 (s, $C^{13'}$), 124.7 (br s, $C^{3'}$, $C^{8'}$, $C^{10'}$, $C^{15'}$, $C^{16'}$), 125.7 (s, $C^{9'}$), 126.6 (s, C_0^3 and $C^{5'}$), 127.3 (m, $C^{2'}$, $C^{6'}$, $C^{12'}$), 128.3 (m, C_m, C_1^3, C_2^3, C^3), 129.4−130.3 (m, $C^{7'}$, $C^{14'}$, C^4), 130.8 (d, $^2J_{CP}$ = 12 Hz, C_o), 131.3 (s, C_3^3), 131.6−132.8 (m, $(HC=N)_0$, C_1^4, C_2^4, $C^{4'}$, C_o, C_p), 133.5 (s, C_0^4, C_3^4), 135.9 (s, $C^{1'}$), 139.7 (br d, $^3J_{cp}$ = 14 Hz, $(HC=N)_1$ and $(HC=N)_2$), 142.0 (s, CH=N), 149.6 (br s, C_0^1), 151.5 (d, $^2J_{CP}$ = 7 Hz, C_2^1), 152.9 (br d, $^2J_{CP}$ = 9 Hz, C^1, C_1^1), 155.0 (d, $^2J_{cp}$ = 7 Hz, C_3^1), 175.9 (s, C=O), 190.7 (s, CHO); $C^{11'}$, CH_2P and C_i not detected. Anal. Calcd for $C_{1074}H_{900}N_{123}O_{162}P_{57}S_{42}$ (21234): C, 60.75; H, 4.27; N, 8.11. Found: C, 60.68; H, 4.20; N, 8.05.

^{31}P NMR is an extraordinary tool for the characterization of phosphorus-containing dendrimers as we have demonstrated in some of our papers.[6,9] It allowed us to follow rigorously the construction of dendrimers since generally up to generation 6 the signal of the phosphorus atom of the core can be detected; lack of substitution on the surface at one or several of the terminal functional groups from generation 1−6 would thus be observed. Moreover, each generation gave a different chemical shift. Furthermore, substitution reactions on the surface generally resulted in a shielding or deshielding effect (depending on the type of substitution) of the signal due to the phosphorus atom of the top generation (n) and a slight deshielding effect for the phosphorus atoms of generation n − 1. In the case of dendrimers reported in this work, the following ^{31}PNMR chemical shift transformations were observed when we were moving from compound **8** to **9**, **10**, and finally **11** (see numbering scheme herewith).

Scheme 2. Multistep Synthesis of the Multilabeled Dendrimer 11

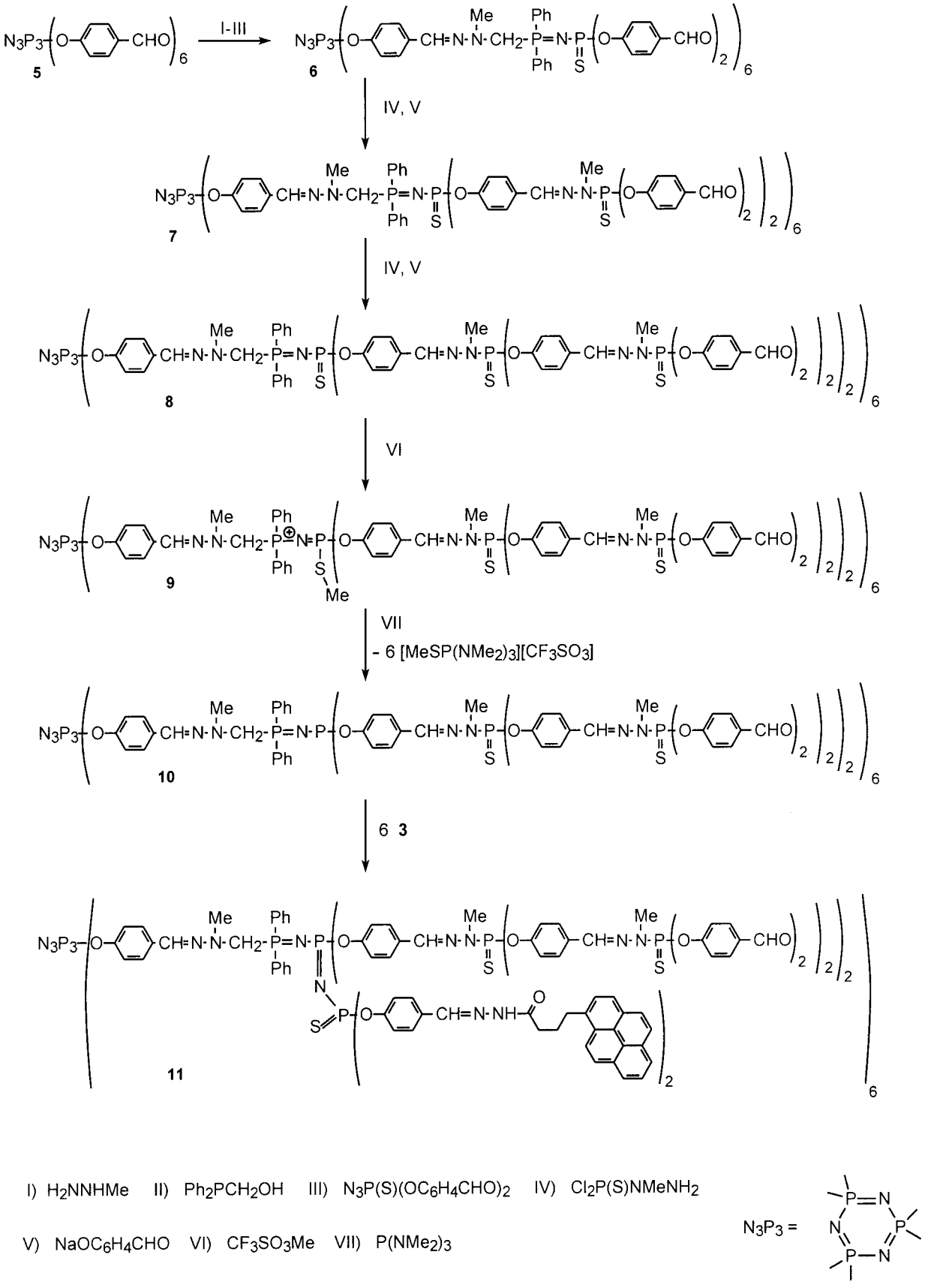

Compound **8:** three singlets are observed at 8.1 (P_0), 60.4 (P_3), and 62.5 (P_2) ppm and two doublets corresponding to the P═N−P═S units at 13.6 (J_{pp} = 31 Hz, P_0') and 52.6 (J_{pp} = 31 Hz, P_1).

Compound **9** was formed by alkylation of the P═N−P═S fragment with CF_3SO_3Me. We observed again three singlets at 8.1 (P_0), 60.6 (P_3), and 62.4 (P_2) ppm and two new doublets at 20.1 (J_{pp} = 9 Hz, P_1) and 24.3 (J_{pp} = 9 Hz, P_0') with the

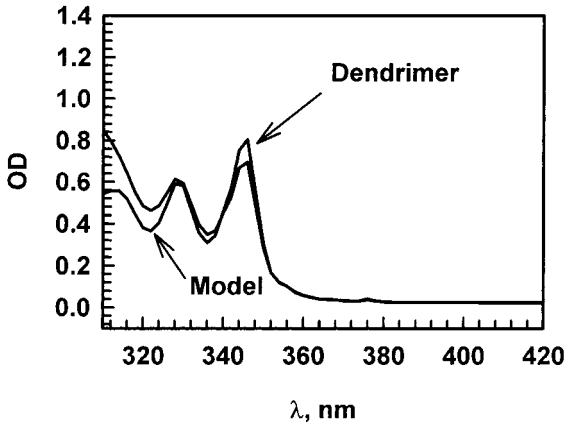

Figure 1. Absorption spectra of model and labeled dendrimers in triethylene glycol. Concentrations: [model] = 3.74×10^{-6} mol/L, [dendrimer] = 1.82×10^{-7} mol/L.

complete disappearance of the previous doublets due to derivative **8**.

Compound **11** was formed by adding an excess of phosphine $P(NMe_2)_3$ to **9**, which allowed the cleavage of the P−SMe bond in **9** with formation of the phosphonium salt $[MeSP(NMe_2)_3]^+$-$CF_3SO_3^-$ and the formation of internal aminophosphite groups. Addition of the azide **3** takes place on these aminophosphite groups. As a result, we could observe clearly in ^{31}P NMR the following chemical shifts: three singlets at 8.1 (P_0), 60.4 (P_3), and 62.4 (P_2) ppm, a doublet of doublet due to the phosphorus P_1 (which is coupled to P_0' and P_1') at −12.5 ($J_{P1P0'}$ = 21 Hz, $J_{P1P1'}$ = 64 Hz), and two doublets at 13.4 ($J_{P1P0'}$ = 21 Hz, P_0') and 46.7 ($J_{P1P1'}$ = 64 Hz). No traces of other signals were detected. Therefore, it is quite reasonable to say that the synthesis of **11**, a dendrimer of generation 3, was complete (**11** was purified by SEC).

Absorption and stationary emission spectra were registered using a Hewlett-Packard 8452A diode array spectrometer and Perkin-Elmer LS 50, respectively. For registration of decay curves we used a setup combining a nitrogen laser (Laser Photonics, USA, model LN 120C; energy up to 78 μJ in the 0.3 ns pulse, λ = 337.1 nm), optical filters used to eliminate reflections of the laser light onto the monochromator slit, a monochromator (Bausch & Lomb (1350 grooves/mm), slit setting 0.1) to select wavelength of emitted light, a detector (Hamamatsu 1P28 or R5600 photomultipliers), a digitizing oscilloscope (Hewlett-Packard 5451 A, 1 Gsa/s) for signal recording, and an IBM-compatible computer for data storage an analysis. All measurements were performed at room temperature, and samples were deareated with nitrogen for 40 min.

Results and Discussion

Absorption Spectra. Positions of absorption maxima and line widths in UV spectra of compounds containing chromophores often depend on the nature of environment of the light-absorbing groups. In the case of pyrene labels absorption spectroscopy was used as an auxiliary tool for detection of pyrene−pyrene ground-state dimers formed in some pyrene-labeled polymers.[10,11]

We noticed that absorption maxima in UV spectra of the model **4** in triethylene glycol were shifted to red by 4 nm in comparison with spectra of the same compound in acetonitrile. Apparently, triethylene glycol, known to complex efficiently ionic and polar species, interacts more effectively with pyrene in excited state than in its ground form. It was worth to note, however, that in absorption spectra of the dendrimers **11** and the model **4** (cf. Figure 1) in the range from 320 to 380 nm positions of all maxima were identical. We considered this observation to be a strong evidence allowing to exclude formation of pyrene−pyrene ground-state dimers enforced by label−dendrimer interactions. It is worth to remember that in the case of 1,3-di(1-pyrenyl)propane probe incorporated into human serum albumin (a natural carrier of hydrophobic compounds) interactions between the bispyrene probe and the host macromolecule resulted in effective formation of the ground-state pyrene−pyrene dimers.[11]

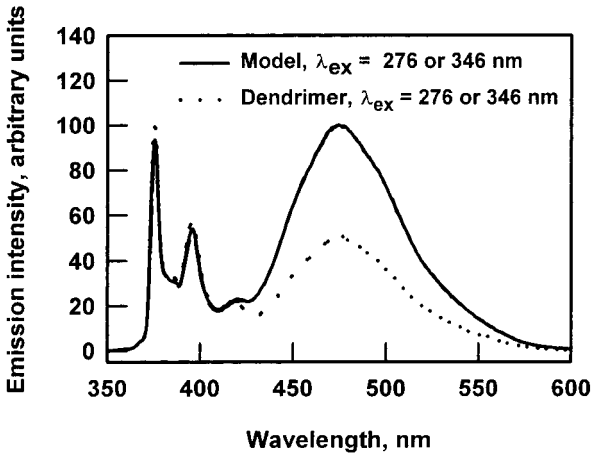

Figure 2. Steady-state emission spectra of model and labeled dendrimers in acetonitrile.

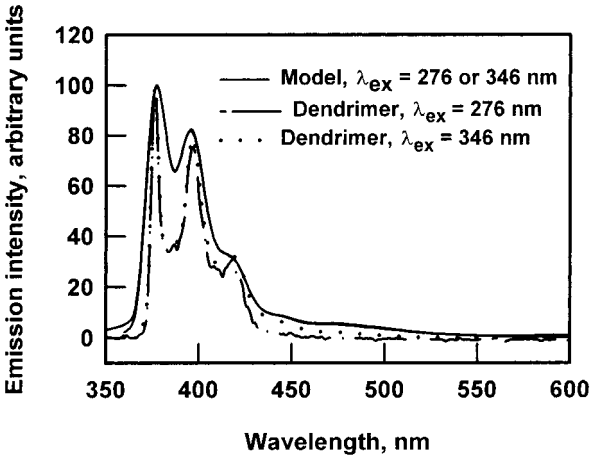

Figure 3. Steady-state emission spectra of model and labeled dendrimers in triethylene glycol.

Steady State of Emission Excitation Spectra of 4 and 11. Emission spectra of **4** and **11** in acetonitrile, diglyme, 1,4-dioxane, triethylene glycol, and cyclohexanol (in the latter only the model could be dissolved) were typical for many pyrene-labeled compounds. Each spectrum was composed of the structured emission from the excited pyrene fluorophores (in the range from 360 to 430 nm) and of the broad emission signal due to the emission from the pyrene−pyrene excimers (maximum at 480 nm). In solvents with low viscosity the intensity of emission at 480 nm was much stronger than in the much more viscous solvents, indicating that in the former ones the steady-state concentrations of excimers were higher. Examples are shown in Figures 2 and 3.

Almost identical emission spectra for samples excited at 276 and 346 nm (cf. Figures 2 and 3) were considered as arguments suggesting the absence of the ground-state pyrene−pyrene dimers in model compound and in dendrimers. However, the above-mentioned preassociation of pyrene moieties was finally excluded on the basis of the excitation spectra that were essentially identical when the intensities of monomer (at 376 nm) and

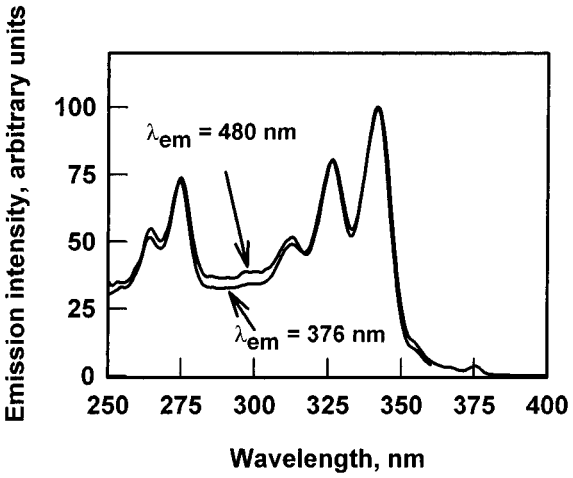

Figure 4. Excitation spectra of model in acetonotrile. Emissions at 376 nm (pyrene monomer) and at 480 nm (pyrene excimer).

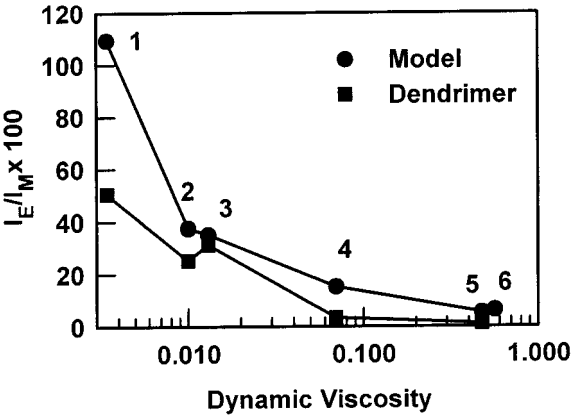

Figure 5. Dependence of the ratio of pyrene excimer and monomer emissions in model compound and in labeled dendrimers on solvent viscosity. Solvents: acetonitrile (1), diglyme (2), 1,4-dioxane (3), 1:1 v:v mixture of 1,4-dioxane and triethylene glycol (4), triethylene glycol (5), cyclohexanol (6).

excimer (at 480 nm) emissions were monitored. An example is given in Figure 4.

Identical excitation spectra of pyrene monomer moieties and pyrene−pyrene excimers indicated that these species were formed by excitation of the same species, the isolated pyrene groups. It is worth noting that in our earlier studies of human serum albumin bearing the 1,3-di(1-pyrenyl)propane probe we found that a higher intensity of excimer emission from samples excited with longer wavelength was due to excitation of the pyrene−pyrene ground-state dimers.[11]

The dependence of the ratio of the intensities of excimer and monomer emissions (I_E/I_M; I_M denotes the intensity of monomer emission at 378 nm whereas I_E the excimer emission at 480 nm) on solvent viscosity registered for the model and labeled dendrimer solutions is shown in Figure 5. I_E was evaluated from the spectra corrected by subtracting from the original one the emission spectrum of 1-pyrenebutyric acid methyl ester used as a model with one pyrene substituent. The analyzed spectra and spectrum of 1-pyrenebutyric acid methyl ester were normalized at 378 nm.

For both investigated compounds I_E/I_M increased significantly with decreasing solvent viscosity. This means that in solvents with low viscosity the steady-state excimer concentration was high. We would like to stress that with exception of acetonitrile in all other

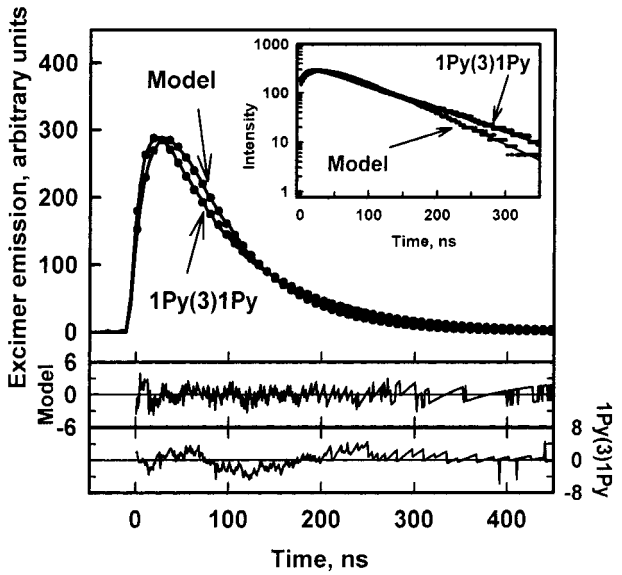

Figure 6. Decay curves of pyrene excimer emission (at 480 nm) in model compound and in 1,3-di(1-pyrenlyl)propane (1Py-(3)1Py). Solvent: 1,4-dioxane. Lines represent experimental traces. Points were calculated on the basis of fits to biexponential equation (for clarity, only every tenth point is shown).

Table 1. I_{III}/I_I Ratio for Model Compound 4 and for Dendrimer 11 in Solvents with Various Dielectric Constant

		I_{III}/I_I	
solvent	D	model	dendrimer
1,4-dioxane	2.21	0.610	0.624
diglyme	7.15	0.560	0.551
cyclohexanol	15.54	0.581	
triethylene glycol	23.40	0.825	0.794
acetonitrile	38.00	0.577	0.570

solvents values of I_E/I_M for model compound and for dendrimer were very close. Close values of I_E/I_M for two systems suggested that the ratio of characteristic time constants for excimer and monomer decays was also close for these systems. (In particular cases it is possible that these time constants do not change when the system is changed.) Further analysis of relation between rates of excimer formation and solvent viscosity will be presented in subsection on decay curves.

It was very well-known that in the pyrene monomer emission spectra (pyrene and/or 1-pyrene linked via propyl spacer to macromolecules) the ratio of emission intensities for the band (0,0) at 378 nm (I_I) and for the band (0,2) at 396 nm (I_{III}) is different for protic and aprotic solvents.[12−15] Thus, it was interesting to check to what extent incorporation of the bispyrene label into the phosphorus-containing dendrimer affects pyrene−solvent interactions. Values of I_{III}/I_I are collected in Table 1.

It was found that values of I_{III}/I_I could not be correlated with solvent polarity characterized by the solvent's dielectric constant. They did not differ significantly also for solutions in aprotic solvents and in cyclohexanol; however, for solutions in triethylene glycol I_{III}/I_I was much higher (cf. Table 1). Nevertheless, even for the latter solvent the values of I_{III}/I_I for model compound and for dendrimer were very close.

Decay Curves. Figure 6 illustrates decays of excimer emission for the model **4** and for 1,3-di(1-pyrenyl)-propane.

Spectra of 1,3-di(1-pyrenyl)propane were analyzed previously.[16] Authors concluded that 1,3-di(1-pyrenyl)-

Scheme 3. Fluorescent Process for 4 and 1,3-Di(1-pyrenyl)propane

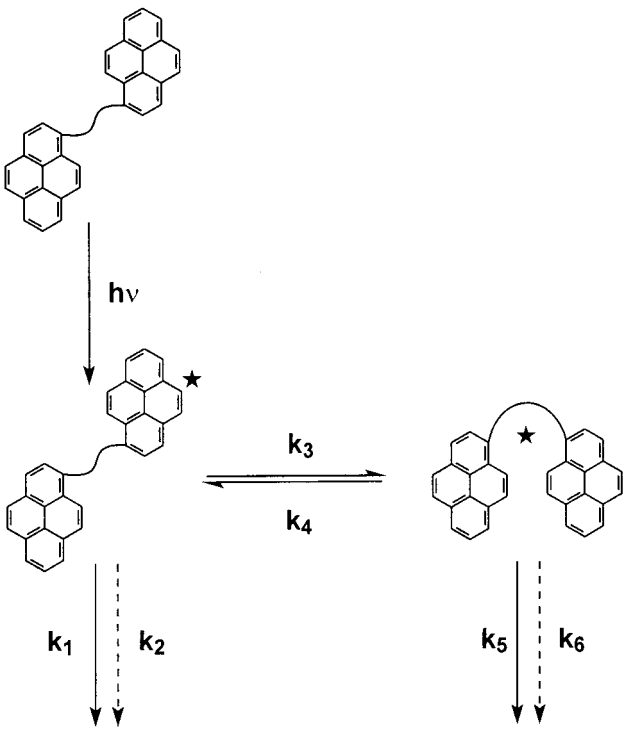

propane upon excitation can form two conformationally different excimers with different lifetimes. However, for practical application of 1,3-di(1-pyrenyl)propane as a probe measuring local microfluidity of its environment such subtle discrimination between the mentioned two kinds of excimers was not necessary, and emission decays were fitted with good approximation with biexponential functions[11] conforming to the Birks scheme (Scheme 3).[17]

In Scheme 3 rate constants k_1 and k_2 denote the radiative and nonradiative deactivation of pyrene monomers, respectively, k_5 and k_6 denote the rate constants of the radiative and nonradiative deactivation of excimer, k_3 denotes the rate constant of excimer formation, and k_4 is the rate constant of decomposition of the excimer to pyrene groups, one in excited and the other in the ground state.

Emission decays of pyrene monomer (I_M) and pyrene−pyrene excimers (I_E) can be described by following set of formulas:

$$I_M = A_{M1}\exp(-t/\tau_1) + A_{M2}\exp(-t/\tau_2) \quad (1)$$

$$I_E = -A_{E1}\exp(-t/\tau_1) + A_{E2}\exp(-t/\tau_2) \quad (2)$$

$$\frac{1}{\tau_{1,2}} = \Big(k_1 + k_2 + k_3 + k_4 + k_5 + k_6 \pm \sqrt{(k_1 + k_2 + k_3 - k_4 - k_5 - k_6)^2 - 4k_3k_4}\Big)/2 \quad (3)$$

Plots in Figure 5 indicated that decay curves for **4** could be fitted with biexponential function with E_2/E_1 close to 1 (as it is needed for Birks scheme), similarly as in the case of 1,3-di(1-pyrenyl)propane. However, it was found that the time constant for excimer formation in **4** was longer than for 1,3-di(1-pyrenyl)propane. This difference was expected because in average the distance between pyrene groups in **4** was larger than in much smaller 1,3-di(1-pyrenyl)propane. Thus, spectra of **4** did not show any unusual features, and therefore it was justified to use this compound as a label probing segmental mobility within dendrimers.

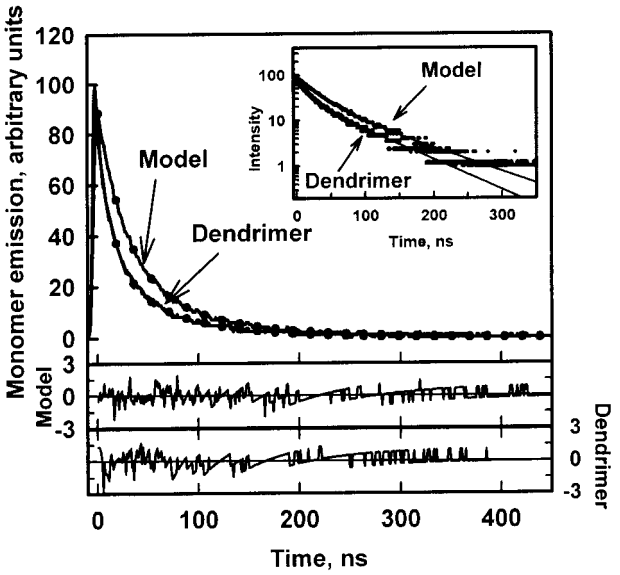

Figure 7. Decay curves of pyrene monomer emission (at 378 nm) in model compound and in labeled dendrimers. Solvent: 1,4-dioxane. Lines represent experimental traces. Points were calculated on the basis of fits to biexponential equation (for clarity, only every tenth point is shown).

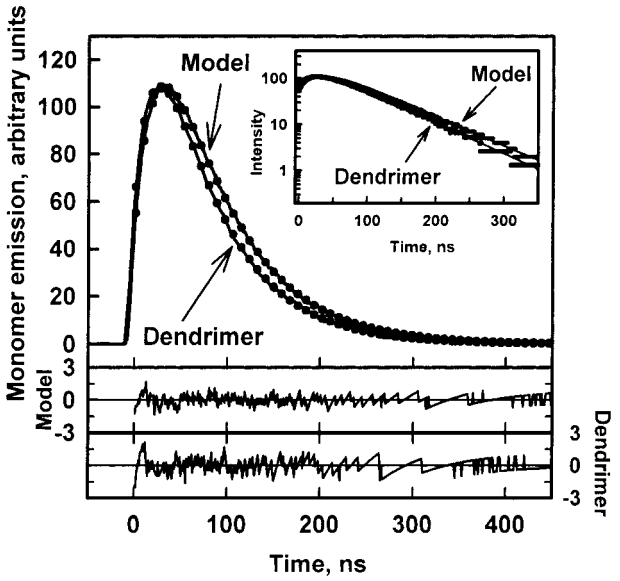

Figure 8. Decay curves of pyrene excimer emission (at 480 nm) in model compound and in labeled dendrimers. Solvent: 1,4-dioxane. Lines represent experimental traces. Points were calculated on the basis of fits to biexponential equation (for clarity, only every tenth point is shown).

Examples of decay curves for monomer and excimer emissions for model compound and for dendrimer **11** are given in Figure 7 and Figure 8. For both these species the emission decays were successfully fitted with biexponential function. Values of τ_1, τ_2, and values of the ratio of preexponential factors for excimer decays (E_2/E_1) in various solvents are listed in Table 2. It is worth noting that for model and for dendrimers E_2/E_1 was only slightly lower than 1. Winnik made similar observation for emission of polystyrenes labled at both ends with pyrene groups (pyrenes substituted at 1 position) and attributed it to small contribution of pyrene monomer emission at longer wavelengths.[18] It is important to

Table 2. Values of the Fluorescence Emission Decay Time Constants for Model 4 and Dendrimer 11

	model			dendrimer			$1/\tau_1$(dendrimer) −
solvent	E_2/E_1[a]	τ_1 (ns)	τ_2 (ns)	E_2/E_1	τ_1 (ns)	τ_2 (ns)	$1/\tau_1$(model) s^{-1}
acetonitrile	0.998	7.1	74.1	0.984	6.2	61.3	2.5×10^7
diglyme	0.876	34.2	68.3	0.852	31.4	56.1	2.5×10^6
1,4-dioxane	0.998	25.3	68.8	1.07	21.8	66.4	6.3×10^6
triethylene glycol	0.883	40.1	110.2	0.976	36.4	117.4	2.5×10^6
cyclohexanol	0.995	34.7	124.3				

[a] Experimental data fitted to the equation $I_E = -A_{E1} \exp(-t/\tau_1) + A_{E2} \exp(-t/\tau_2)$.

stress that values of E_1/E_2 close to 1 indicate the absence of the pyrene−pyrene ground-state dimer.

It has been found that for pyrene substituted at position 1 with propyl linker the rate constant of excimer decomposition to excited and nonexcited pyrene groups (k_4) is very low. For example, in the case of polystyrene molecules substituted at both ends with pyrene groups, in cyclohexane and in toluene, at room temperature, $1/\tau_1$ and $1/\tau_2$ could be approximated by putting in formula 3 k_4 equal to zero.[17,18] At such approximation

$$\frac{1}{\tau_1} = k_1 + k_2 + k_3 \tag{4}$$

$$\frac{1}{\tau_2} = k_5 + k_6 \tag{5}$$

Similar values of τ_2 for model and for dendrimer emissions in each solvent indicate that rate constants of the radiative (k_5) and nonradiative (k_6) deactivation of excimer do not differ substantially for these two species. Moreover, changes of solvent from triethylene glycol to acetonitrile, diglyme, or 1,4-dioxane resulted in an increase of $k_5 + k_6$ by ca. 40%. It is reasonable to assume that also for excited pyrene groups the similar relation would hold (k_1(model) + k_2(model) ≅ k_1(dendrimer) + k_2(dendrimer)). Using eq 4 and the above assumption, the difference of rate constants of excimer formation in dendrimer and in model (Δk_3) can be estimated from the following relation:

$$\Delta k_3 = \frac{1}{\tau_2(\text{dendrimer})} - \frac{1}{\tau_2(\text{monomer})}$$

It is worth noting that for investigated solvents values of $1/\tau_2$(dendrimer) − $1/\tau_2$(model) varied from 2.5×10^6 to 2.0×10^7 s^{-1} (cf. Table 2).

In triethylene glycol $0 < k_1 + k_2 \leq 2.7 \times 10^7$ s^{-1} (τ_2 equals to 40.1 and 36.4 ns in model and in dendrimer, respectively). Assuming that in acetonitrile, diglyme, and 1,4-dioxane the radiative and nonradiative deactivation rate constants for excited pyrene moieties differ from that in triethylene glycol similarly as deactivation rate constants for excimer (i.e., by ca. 40%) $0 < k_1 + k_2 \leq 3.8 \times 10^7$ s^{-1} in these solvents. Remembering that $k_3 = 1/\tau_2 - (k_1 + k_2)$ and that in acetonitrile $1/\tau_2$ equals 1.6×10^8 and 1.7×10^8 s^{-1} (for model and dendrimer, respectively) k_3 has to be in the limits 1.2×10^8 $s^{-1} < k_3$(model) $< 1.6 \times 10^8$ s^{-1} and 1.3×10^8 $s^{-1} < k_3$(dendrimer) $< 1.7 \times 10^8$ s^{-1}. Thus, in acetonitrile $\Delta k_3 = 2.0 \times 10^7$ s^{-1} for dendrimer, and the model constitutes a relatively small difference.

The above estimate of $k_1 + k_2$ in the model compound and in dendrimer was reasonable remembering that for 1-pyrenebutyric acid methyl ester $k_1 + k_2$ in acetonitrile, 1,2-dimethoxyethane, and 1,4-dioxane was found to be equal 6.4×10^6, 5.5×10^6, and 5.5×10^6 s^{-1}, respectively.[20]

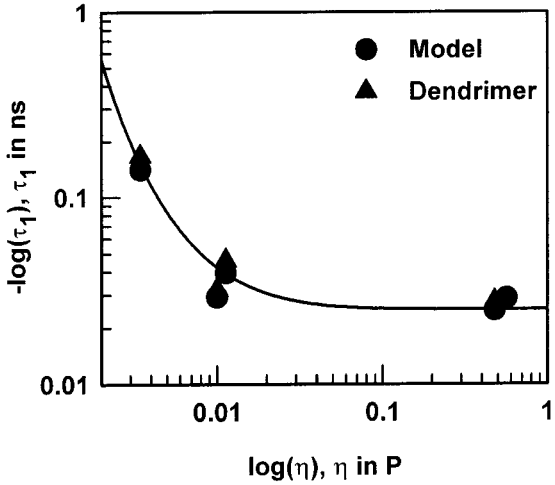

Figure 9. Dependence of −log(τ_1) on solvent viscosity.

The relation between the time constant of excimer emission buildup (τ_1) and solvent viscosity is shown in Figure 9. For both model and dendrimers, the increased solvent viscosity resulted in lower values of $1/\tau_1$, i.e., in lower values of $k_1 + k_2 + k_3$. It is worth noting that whereas changes of solvent from acetonitrile to triethylene glycol resulted in ca. 6-fold decrease of $k_1 + k_2 + k_3$ the estimated decrease of $k_1 + k_2$ was only by ca. 40% (assuming that the deactivation rate constants for excited pyrene monomer ($k_1 + k_2$) and excimer ($k_5 + k_6$) change to a similar degree in various solvents.) Thus, for the considerable decrease of $k_1 + k_2 + k_3$ responsible was the decrease of k_3. Therefore, we may conclude that in the more viscous solvents the pyrene labels move slower (k_3 decreases). Apparently, molecules of solvents used in our studies very efficiently penetrated interior of dendrimers and determined mobility of segments labeled with pyrene fluorophores.

Slightly lower values of $1/\tau_2$ for dendrimers than for the model are probably due to faster nonradiative decay for pyrene fluorophores in the former compound, resulting from interactions with dendrimer segments.

In conclusion, the combined results of analysis of absorption, stationary emission, and excitation spectra as well as analysis of emission decays of model and dendrimers allow us to exclude formation of ground-state pyrene−pyrene dimers in investigated species. Moreover, the stationary emission spectra and emission decays indicate that molecules of acetonitrile, diglyme, 1,4-dioxane, and triethylene glycol constitute the nearest environment of pyrene-labeled segments of the dendrimer of generation 3 determining their segmental mobility at the G_0 level. Movements of the internal pyrene groups were not hindered by interactions with branches of the dendrimers.

Acknowledgment. This work was completed with support of the European Associated Laboratory financed by Polish Committee for Scientific Research and French Centre National de la Recherche Scientifique.

References and Notes

(1) Caminati, G.; Turro, N. J.; Tomalia, D. A. *J. Am. Chem. Soc.* **1990**, *112*, 8515−8522.
(2) Wade, D. A.; Torres, P. A.; Tucker, S. A. *Anal. Chim. Acta* **1999**, *397*, 17−31.
(3) Pistolis, G.; Malliaris, A.; Tsiourvas, D.; Paleos, C. M. *Chem. Eur. J.* **1999**, *5*, 1440−1444.
(4) Hofkens, J.; Latterini, L.; De Belder, G.; Gensch, T.; Maus, M.; Vosch, T.; Karni, Y.; Schweitzer, G.; De Schryver, F. C.; Hermann, A.; Müllen, K. *Chem. Phys. Lett.* **1999**, *304*, 1−9.
(5) Karni, Y.; Jordens, S.; De Belder, G.; Schweitzer, G.; Hofkens, J.; Gensch, T.; Maus, M.; De Schryver, F. C.; Hermann, A.; Müllen, K. *Chem. Phys. Lett.* **1999**, *310*, 73−78.
(6) Galliot, Ch.; Larré, Ch.; Caminade, A.-M.; Majoral, J.-P. *Science* **1997**, *277*, 1981−1984.
(7) Cave, C.; Galons, H.; Miocque, M.; Ringard, P.; Tran, G.; Binet, P. *Eur. J. Med. Chem.* **1990**, *25*, 75−79.
(8) Mitjaville, J.; Caminade, A.-M.; Mathieu, R.; Majoral, J.-P. *J. Am. Chem. Soc.* **1994**, *116*, 5007−5008.
(9) Launay, N.; Caminade, A.-M.; Lahana, R.; Majoral, J.-P. Angew. *Chem., Int. Ed. Engl.* **1994**, *33*, 1589−15992.
(10) Winnik, F. M. *Chem. Rev.* **1993**, *93*, 587−614.
(11) Kowalczyk, D.; Wolszczak, M.; Slomkowski, S. *Colloid Polym. Sci.* **1997**, *275*, 99−105.
(12) Kalayanasundaram, K.; Thomas, J. K. *J. Am. Chem. Soc.* **1977**, *99*, 2039−2044.
(13) Turro, N. J.; Baretz, B. H.; Kuo, P.-L. *Macromolecules* **1984**, *17*, 1321−1324.
(14) Winnik, F. M.; Winnik, M. A.; Tazuke, S. *J. Phys. Chem.* **1987**, *91*, 594−597.
(15) Ringsdorf, H.; Venzmer, J.; Winnik, F. M. *Macromolecules* **1991**, *24*, 1678−1686.
(16) Zachariasse, K. A.; Kühnle; Leinhos, U.; Reynders, P.; Striker, G. *J. Phys. Chem.* **1991**, *95*, 5476−5488.
(17) Klöpfer, W. In *Organic Molecular Photophysics*; Birks, J. B., Ed.; Wiley: London, 1973; Vol. 1, p 357.
(18) Winnik, M. A.; Redpath, A. E. C.; Paton, K.; Danhelka, J. *Polymer* **1984**, *91*, 91−99.
(19) Winnik, M. A. In *Photophysical and Photochemical Tools in Polymer Science; Conformations, Dynamics, Morphology*; Winnik, M. A., Ed.; D. Reidel Publ. Co.: Dordrecht, 1985; p 293.
(20) Cheung, S.-T.; Winnik, M. A.; Redpath, A. E. C. *Makromol. Chem.* **1982**, *183*, 1815−1824.

MA0020077